

MM, FILE COPY

(4)

AD-A203 385

OFFICE OF NAVAL RESEARCH
CONTRACT N00014-81-C-0776
TASK No. NR 051-775
TECHNICAL REPORT #35

AN IN-SITU GRAZING INCIDENCE X-RAY SCATTERING STUDY OF THE
INITIAL STAGES OF ELECTROCHEMICAL GROWTH OF LEAD
ON SILVER (III)

by

O.R. Melroy*, M.F. Toney*, G.L. Borges*, M.G. Samant*,
J.B. Kortright**, P. Ross**, and Leser Blum***

*IBM Almaden Research Center
650 Harry Road
San José, CA 95120

**Lawrence Berkeley Laboratory
Berkeley, CA 94720

***Physics Department, University of Puerto Rico
Rio Piedras 00931

Prepared for Publication in the Journal of
Electroanalytical Chemistry

SDTIC
ELECTE
DEC 15 1988
E

Reproduction in whole or in part is permitted for
any purpose of the United States Government

*This document has been approved for public release
and sale, its distribution is unlimited

*This statement should also appear in Item 10 of Document
Control Data - DD Form 1473. Copies of form available from
cognizant contract administrator.

8 8 12 14 053

Unclassified

ADA20385

SECURITY CLASSIFICATION OF THIS PAGE (When Data Entered)

REPORT DOCUMENTATION PAGE		READ INSTRUCTIONS BEFORE COMPLETING FORM
1. REPORT NUMBER Technical Report #35	2. GOVT ACCESSION NO.	3. RECIPIENT'S CATALOG NUMBER
4. TITLE (and Subtitle) An In-Situ Grazing Incidence X-ray Scattering Study of the Initial Stages of Electrochemical Growth of Lead on Silver(III)	5. TYPE OF REPORT & PERIOD COVERED Interim Technical Report	
	6. PERFORMING ORG. REPORT NUMBER	
7. AUTHOR(s) O.R. Melroy, M.F. Toney, G.L. Borges, M.G. Samant, J.B. Kortright, P.M. Ross, and Lesser Blum	8. CONTRACT OR GRANT NUMBER(s) 00014-81-C-0776	
9. PERFORMING ORGANIZATION NAME AND ADDRESS Department of Physics University of Puerto Rico Box AT, Río Piedras, P.R. 00931	10. PROGRAM ELEMENT, PROJECT, TASK AREA & WORK UNIT NUMBERS	
11. CONTROLLING OFFICE NAME AND ADDRESS Code 472 Office of Naval Research Arlington, VA 22217	12. REPORT DATE 11-5-88	
	13. NUMBER OF PAGES 21	
14. MONITORING AGENCY NAME & ADDRESS (if different from Controlling Office)	15. SECURITY CLASS. (of this report) unclassified	
	15a. DECLASSIFICATION/DOWNGRADING SCHEDULE	
16. DISTRIBUTION STATEMENT (of this Report) Approved for public release; Distribution Unlimited		
17. DISTRIBUTION STATEMENT (of the abstract entered in Block 20, if different from Report)		
18. SUPPLEMENTARY NOTES Prepared for publication in the Journal of Electroanalytical chemistry.		
19. KEY WORDS (Continue on reverse side if necessary and identify by block number) (Electrochemical growth, x-ray diffraction, electrode surfaces.)		
20. ABSTRACT (Continue on reverse side if necessary and identify by block number) The potential dependent structure of underpotentially deposited lead on silver(III) and the initial stages of bulk lead deposition on the ad-layer have been studied using grazing incidence x-ray scattering. Measurements were made in-situ and under potential control. The closed packed triangular lattice of lead formed by the underpotential deposition (at full monolayer coverage) is compressed 1.4% relative to bulk lead. This compressive strain increases linearly with applied potential until the onset of bulk deposition where the		

ND FORM 1473
1 JAN 73

EDITION OF 1 NOV 63 IS OBSOLETE
S/N 0102-LF-014-6601

Unclassified

SECURITY CLASSIFICATION OF THIS PAGE (When Data Entered)

UNCLASSIFIED

SECURITY CLASSIFICATION OF THIS PAGE (When Data Entered)

ad-layer is compressed 2.8%. Bulk lead is not deposited epitaxially on this template because of the large compressive strain. Instead, it grows as islands that have (111) texture but are randomly oriented in the plane of the substrate. After the deposition of approximately five equivalent monolayers of bulk lead, the initial ad-layer appears to reconstruct.

Accession For	
NTIS GRA&I	<input checked="" type="checkbox"/>
DTIC TAB	<input type="checkbox"/>
Unannounced	<input type="checkbox"/>
Justification	
By	
Distribution/	
Availability Codes	
Dist	Avail and/or Special
A-1	



UNCLASSIFIED

SECURITY CLASSIFICATION OF THIS PAGE (When Data Entered)

**An In-Situ Grazing Incidence X-ray Scattering Study of the
Initial Stages of Electrochemical Growth of Lead on Silver (111)**

O.R. Melroy, M.F. Toney, G.L. Borges, and M.G. Samant

IBM Almaden Research Center
650 Harry Road
San Jose, CA. 95120

J. B. Kortright and P.N. Ross

Lawrence Berkeley Laboratory
University of California
Berkeley, CA 94720

L. Blum

Physics Department ;
College of Natural Sciences
P.O. Box AT
Rio Piedras, Puerto Rico 00931

ABSTRACT

The potential dependent structure of underpotentially deposited lead on silver (111) and the initial stages of bulk lead deposition on the ad-layer have been studied using grazing incidence x-ray scattering. Measurements were made in-situ and under potential control. The closed packed triangular lattice of lead formed by the underpotential deposition (at full monolayer coverage) is compressed 1.4% relative to bulk lead. This compressive strain increases linearly with applied potential until the onset of bulk deposition where the ad-layer is compressed 2.8%. Bulk lead is not deposited epitaxially on this template because of the large compressive strain. Instead, it grows as islands that have (111) texture but are randomly oriented in the plane of the substrate. After the deposition of approximately five equivalent monolayers of bulk lead, the initial ad-layer appears to reconstruct.

INTRODUCTION

Understanding the structure of electrochemical surfaces and adsorbed layers is fundamental both to understanding their chemical reactivity and the growth of any material that is subsequently deposited. Considerable effort has been directed toward determining the structure of the first adsorbed layer using well established electrochemical techniques,¹ spectroscopic measurements such as specular reflectance,² second harmonic generation,³ x-ray standing wave,⁴ surface EXAFS,^{5,6} and others,⁷⁻¹⁰ as well as standard surface science methods following transfer of the substrate into ultrahigh vacuum.^{11,12} The relationship between the initial ad-layer and subsequent growth, however, has been studied in far less detail. This lack of information is largely a result of the lack of experimental techniques capable of microscopically probing the initial stages of growth in-situ.

In contrast, a substantial body of information exists on vacuum deposition and epitaxial growth.¹³ Several researchers have considered the influence of substrate-adsorbate and adsorbate-adsorbate interactions on the growth mode of physisorbed gases and developed theories to predict when layer-by-layer growth (Frank-van der Merwe) or the formation of bulk islands on top of one or more layers (Stranski-Krastanov) will occur.¹⁴ More recent theories have also identified compressive strain in the initial layers resulting from a large substrate-adsorbate interaction as a critical parameter.^{15,16} Although in electrochemical deposition, the adsorption of the solvent and electrolyte are known to have a pronounced effect, many of the ideas developed for vacuum deposition may be relevant to electrochemical growth. To apply these ideas, however, measurements of the strain of the interfacial layer as well as the microscopic structure of the initial stages of subsequent growth are required.

X-ray spectroscopies are ideally suited to the study of the metal/solution interface. X-rays have a significant penetration depth in condensed phases and because their wavelength is on the same order as interatomic distances, provide direct geometrical information. X-ray diffraction is among the best developed x-ray technique and has been used by several groups to probe electrochemical processes.¹⁷⁻²¹ X-rays, however, have relatively low cross sections and thus largely have been limited to studying

relatively thick samples ($> 100 \text{ \AA}$). The availability of synchrotron radiation, five orders of magnitude more intense than conventional sources, now allows x-ray spectroscopies to be applied successfully to monolayer films.^{17,18}

Grazing incidence x-ray scattering (GIXS) is becoming an established surface science and thin film tool.²²⁻²⁵ In this geometry, the incident beam impinges on the surface near the critical angle for total external reflection. This limits the penetration depth to less than a hundred angstroms and increases the intensity of the electric field at the surface. In an earlier report, this technique was used to determine, in-situ, the structure of an underpotentially deposited layer of lead.^{17,18} In this paper, we have extended these measurements to study the potential dependence of the structure of the ad-layer and the influence of interfacial strain on the subsequent growth of bulk lead.

EXPERIMENTAL

The electrode preparation and electrochemical cell have previously been described in detail^{17,18} so only the key points will be discussed here. The requirements for the x-ray scattering and good thin layer electrochemistry are difficult to meet simultaneously. The critical angle for most metals in the hard x-ray region is about $0.2\text{--}0.5^\circ$, resulting in a long x-ray path through the electrolyte. Therefore, it is essential that the x-ray scattering be measured with only a thin layer of electrolyte covering the electrode to minimize the diffuse background scattering. This shallow angle of incidence coupled with the need for a thin layer cell with an x-ray transparent window accentuates cell resistance problems. As a compromise, the electrochemical cell was designed so that the metal layer could be deposited with a relatively thick layer of electrolyte covering the electrode (and characteristic voltammograms obtained) and then reconfigured to a thin layer cell in which the x-ray scattering was measured. This approach is analogous to that used in infrared absorption experiments at metal/liquid interfaces where similar problems are encountered.¹⁰

The lead monolayer was deposited at -400 mV vs. a Ag/AgCl (3M KCl) reference electrode from a 0.1M sodium acetate, 0.1M acetic acid, and $5 \times 10^{-3} \text{ M}$ lead acetate electrolyte and reconfigured to the

thin layer geometry at this potential. All chemicals were Aldrich ultrapure reagents. Deionized water was obtained from a Barnstead "nanopure" system with an "organopure" attachment. Experiments at different potential were conducted by changing the potential after the cell was in the thin layer configuration. This procedure allows the electrode to be made more negative than the potential for bulk lead deposition without covering the surface with a thick layer of lead since only a relatively small amount of lead is contained in the thin (ca. 1-10 μ) layer of electrolyte. For studies of the initial stages of bulk deposition, a predetermined amount of lead was deposited then solution was removed from the cell leaving only the thin layer covering the surface to minimize additional deposition during the x-ray scattering measurements. However, as much as 1-3 monolayer equivalents of additional bulk lead may have been deposited after reconfiguration.²⁷ To prevent the layer of electrolyte from drying and to avoid complications from the slow oxidation of the lead due to diffusing oxygen, the lead was electrochemically removed and redeposited between diffraction scans for each potential.

The x-ray diffraction data were collected at the Stanford Synchrotron Radiation Laboratory (SSRL) under dedicated beam conditions on a focussed 54-pole wiggler beam line (VI-2). This beam line was equipped with a Huber four circle diffractometer on which the electrochemical cell^{17,18} was mounted with a Huber goniometer head. The sample was held in the vertical plane with the incident angle of x-rays, α , equal to the exit angle, δ , at which the scattered beam was collected. The advantage to the vertical scattering geometry is that the broad direction of the highly anisotropic synchrotron resolution function is aligned along the direction of the Bragg rods from the monolayer.²⁵ This significantly enhances the surface signal. The incident x-ray beam energy was chosen to be 12350 eV (1.003 \AA) using a silicon (220) double crystal monochromator. This x-ray energy was calibrated by measuring the diffraction from a silicon (111) crystal. This x-ray beam size was restricted by slits to 0.5 mm in vertical direction and 2 mm in horizontal direction. The incident beam intensity was measured by a scintillation detector using a kapton film as a beam splitter. The diffracted intensity was measured by a scintillation detector equipped with anti-scatter slits which were nominally set to the same settings as the front slits. The in-plane resolution was approximately 0.005 \AA^{-1} .

RESULTS

The electrochemical deposition of lead onto silver (111) from an acetate electrolyte occurs in two distinct steps. The current response to a linear sweep of potential is shown in figure 1. The first peak at approximately -350mV vs Ag/AgCl corresponds to the deposition of a single monolayer of lead, i.e. the UPD ad-layer.¹ The cathodic wave, and corresponding anodic peak on reversal, represents the transient faradaic currents for the deposition (stripping) of bulk lead in this electrolyte. That this UPD ad-layer is an incommensurate close packed triangular monolayer had been inferred using a variety of techniques^{2,7} and recently has been proven in a *in-situ* x-ray diffraction experiment.^{17,18} Standard coulometric and capacitance measurements indicated that at rest potentials between ca. -400 and -550 mV there were no measurable changes in the coverage by lead, i.e. the coverage remained at essentially one monolayer ($\pm 5\%$). In this potential region, the lead coverage is known to be stable with time, as for example reported by Juttner and co-workers,²⁸ but an instability does appear to occur when the potential is held in the region of submonolayer coverage.²⁸

It is useful to view the GIXS diffraction scans in terms of the equivalent LEED pattern for this surface, which is shown in figure 2. A radial scan corresponds to measuring the intensity along a radial vector (\vec{Q}) starting from the origin. An azimuthal scan (ϕ) corresponds to measuring the intensity along an arc at a fixed distance ($|\vec{Q}| = 4\pi \sin \theta / \lambda$) from the center. An oriented crystal produces spots while a powder creates rings.

As expected, at potentials of -350mV , no scattering from a lead overlayer is observed in the diffraction experiment. One of the silver crystal truncation rods²⁶ measured under these conditions is shown in figure 3. The width of the azimuthal scan shows the in-plane silver mosaic to be 0.15° . The diffuse background scattering is largely due to the layer of solution covering the electrode. At potentials negative of -350mV , the ad-layer is present and lead reflections are observed. A scan of a first order lead reflection with the electrode held at -425mV is shown in figure 4. The peak appears at $|\vec{Q}| = 2.11 \text{ \AA}^{-1}$, corresponding to a lead-lead near neighbor distance of 3.45 \AA . This is a 1.4% compression from the near neighbor distance in bulk lead.

As the potential of the electrode is made more negative, the lead-lead near neighbor distance decreases. (The scattering angle at which the lead reflection is observed increases.) A plot of the lead-lead near neighbor distance vs. electrode potential is shown in figure 5. The near neighbor distance decreases linearly with potential until the onset of bulk deposition. At this potential, the measured near neighbor distance is 3.40 Å, a 2.8% contraction from bulk lead. No additional change in the spacing was observed when the potential was cathodic to the potential for bulk lead deposition.

To study the growth of subsequent layers, bulk lead was electrochemically deposited at a constant potential (following the initial deposition of the monolayer) before reconfiguring the cell to the thin layer geometry. The amount deposited was determined from the electrochemical current. After the deposition of 2-3 equivalent "monolayers" bulk lead²⁷, no change was observed in the scattering from the ad-layer. An "equivalent monolayer" of bulk lead in this context only refers to an amount of lead contained in one geometric monolayer ($300 \mu\text{C}/\text{cm}^2 = 10^{15} \text{ atoms}/\text{cm}^2$). This in no way implies that the lead is grown in a layer by layer manner. That there is no change in the intensity of the lead scattering after deposition of the second "monolayer" shows, in fact, that this layer is not epitaxial with the first layer. If it were, the intensity of the lead reflections would have changed significantly.

No reflections were observed from the additional bulk deposit, which would suggest that these bulk crystallites are somewhat randomly oriented (at least with respect to the azimuthal direction in the plane of the substrate). After the deposition of 5 or more "monolayers"²⁷, the previously observed scattering from the ad-layer disappears. Even at the critical angle, the penetration depth of the x-rays is much greater than the thickness of the lead overlayer. The disappearance of the diffraction peaks from the ad-layer must result from a restructuring of the layer itself. No diffraction from the lead is seen until approximately 100 equivalent monolayers have been deposited. The lead (220) reflection is then observed and is shown in figure 6. The lead-lead near-neighbor distance calculated from these data is 3.50 Å, in good agreement with the spacing in bulk lead. The lead islands are not well oriented in the plane of the substrate, which results in a significant decrease in the signal to noise ratio since the scattering intensity is spread over a large radial arc. If the overlayer were, for example, a (111) textured surface but randomly oriented in the plane of the surface, the signal to noise ratio

would decrease by a factor of about 600. This is consistent with figures 4 and 6, where the measured intensity from the bulk (100 monolayers) is about 1/6 that of the monolayer.

DISCUSSION

It is now well established that at full coverage, underpotentially deposited lead on silver (111) orders into an incommensurate triangular closed packed monolayer. Because lead forms a face centered cubic (fcc) crystal, this monolayer is similar to the lead (111) surface, except for the absence of the underlying lead layers. From this, and since the (111) surface has the lowest surface free energy (for fcc), it would be reasonable to expect bulk lead to grow epitaxially on this template. Clearly, this does not occur. The failure of lead to grow epitaxially appears to be a result of the compressive strain in the first layer.

For layers adsorbed on smooth substrates, the importance of compressive strain on the growth of subsequently adsorbed material has been recognized only recently. Originally, theories suggested that for sufficiently strong adsorbate-substrate interaction relative to the adsorbate-adsorbate interaction layer-by-layer growth would occur,¹⁴ since in this growth mode the number of atoms near the substrate are maximized. However, experiments on inert gases physisorbed on graphite have shown that this is not so.¹⁵ The discrepancy between the theories and these experiments has recently been attributed to the fact that the theories ignored the compression in the layers which results from the strong substrate-adsorbate interaction.^{15,16} The increase in strain energy that would be built up in layer-by-layer growth overwhelms the decrease in energy that results from adsorption near the substrate. This quenches the epitaxy of further layers and results in the growth of bulk crystallites.

Although these theories were developed for physisorption and the detailed calculations are not applicable in our case, the idea that compressive strain is a determining factor is relevant. The significantly stronger lead-silver interaction compared to the lead-lead interaction¹⁷ causes the large (2.8%) lattice parameter mismatch between the lead monolayer and bulk lead, and results in the Stranski-Krastanov growth mode. It is important to note that the physical origin of the lattice

parameter mismatch that causes lead on silver (111) to grow in the Stranski-Krastanov mode is different from that which causes this growth mode on adlayers where the first monolayer is commensurate. When the first monolayer is commensurate, its lattice spacing is different from that in the bulk since it takes on a lattice spacing simply related to the substrate, and not its natural spacing. Layer-by-layer growth (with all the layers mutually commensurate) is energetically unfavorable, because the lattice parameter mismatch results in a large strain energy. Thus, the growth mode is Stranski-Krastanov as shown for several metal-metal systems²⁷⁻²⁹ and for rare gases on lamellar halides.³⁰ Note that for a commensurate monolayer the lattice parameter mismatch can be either positive (adlayer spacing greater than bulk) or negative (adlayer spacing less than bulk). For lead on silver the monolayer is incommensurate and the lattice mismatch (necessarily negative) is caused by a strong attraction of the adsorbate to the substrate, not a spacing dictated by the substrate.

The bulk lead crystallites grow atop the compressed monolayer. Since the lattice spacing between the two Pb structures are different, there is an interfacial strain. As bulk lead is deposited atop the compressed monolayer the crystallites grow both laterally and vertically, but due to the presence of an attractive substrate, it is likely the growth is primarily lateral.³³ This lateral growth increases the interfacial strain energy, and at some crystallite size this strain energy becomes larger than the energy gained by having extra atoms (compression) in the initial monolayer. At this point, the initial monolayer appears to restructure, perhaps conforming to the structure of the bulk lead atop it. For lead on silver, this crossover occurs after approximately 5 equivalent monolayers of bulk have been deposited. Although the underpotentially deposited monolayer is restructured and the lead randomly oriented in the plane of the substrate, it is not a randomly oriented, polycrystalline film. The observation of the (220) reflection from the lead film (figure 6) shows that it has a (111) fiber texture. (If the film were polycrystalline, the intensity of this reflection would be too weak to be observed for this film thickness.) It seems likely that the restructured first layer is 'epitaxial' with the bulk crystallites and has the same structure as a (111) layer of lead with the bulk spacing.

It is difficult to draw conclusions from comparisons of UPD lead on silver with vacuum deposited lead^{2,35} for several reasons. First, it is important to reiterate some key differences between the two

environments. In vacuum deposition, there is no contribution from adsorbed solvent and (or) electrolyte. In addition, the room temperature deposition of lead in vacuum is inherently a non-equilibrium process. Because of the low vapor pressure of lead, the structure of the deposited lead may be dominated by kinetic limitations (low surface mobility). In contrast, the exchange between lead atoms on the surface and ions in solution is rapid and surface diffusion of the neutral atom should be less important. It is known, for example, that even in the absence of faradaic current, the topography of metal electrodes can change over relatively short times when exposed to electrolytic solutions, particularly those containing strongly adsorbing ions.³⁴ Thus, discrepancies between the electrochemically and vacuum deposited lead may reflect true equilibrium differences in deposition in the two environments or they may result from kinetic limitations for the vacuum deposited layers. The second difficulty is that there does not appear to be a consensus on the growth of vacuum deposited lead on silver (111). Frank-van der Merwe behavior (layer-by-layer growth) was reported in one case,³⁵ while island films (Stranski-Krastanov type growth) were observed following the adsorption of 1.6 monolayers in another.² There are, however, similarities in the growth in the two environments. Both groups have observed that in vacuum, at full coverage, the first layer of lead is a closed packed triangular lattice incommensurate with the silver substrate. This layer was also found to be compressed, although in both cases the observed strain was much less than for electrochemically deposited lead.

The compression of the lead ad-layer with applied potential shown in Figure 4 is not unexpected, but the reason for such expectation is not immediately obvious. To see that this compression might be expected, an analogy to the thermodynamically equivalent system of an adsorbed or condensed gas in equilibrium with the gas vapor is useful. In the case of rare gases adsorbed on graphite, for example, the spacing of the ad-layer was measured³⁶ as a function of the effective gas pressure, and the resulting tangential (2D) compression of the gas monolayer could be used to calculate the 2D compressibility of the gas by application of a straightforward thermodynamic analysis³⁸. Analogously, if the UPD layer is in equilibrium with its ions in solution, then a cathodic overpotential (relative to the potential at which the ad-layer is at unit activity) means that the concentration of ions in equilibrium with the layer at that potential is lower than the concentration in solution, which was fixed experimentally.

There is, therefore, an ionic "overpressure" which is the thermodynamic driving force for 2D compression of the lead monolayer. This driving force exists even if the monolayer is not true equilibrium with the ions in solution.

One reason the importance of strain in the first ad-layer on electrochemical growth has not attracted more attention is that x-ray diffraction is one of the few techniques capable of measuring such small changes. The compression of the monolayer between -400mV and -550mV represents the addition of only $7\mu\text{C}/\text{cm}^2$ of lead. Electrochemically, it is virtually impossible to distinguish this small faradaic charge above the capacitive charging. Likewise, the uncertainties in the electrode area and the electrosorption vacancy are far too large to permit the 1.4% compression upon formation of the underpotentially deposited layer to be observed by measuring the faradaic current associated with the deposition. The compression is also difficult to address using standard ex-situ methods. In addition to questions of possible structural changes when removed from potential control and transfer into UHV, 1% changes in lattice spacings are near the limit of resolution for LEED. As shown above, however, these "small" changes in the lattice spacing may be the dominant force in determining the morphology of subsequent growth. Before the structure of electrochemically deposited metals can be predicted from the properties of the first monolayer, both a greater understanding of the influence of the strain on the initial stages of metal deposition and the influence of the substrate on the strain will be required.

CONCLUSION

We have shown that GDS can be used in situ to study the initial stages of metal electrodeposition on well defined substrates. The underpotential deposition of lead on silver (111) produces a monolayer having a close packed triangular lattice that is compressed 1.4% relative to bulk lead. This compression increased with cathodic potential until the onset of multilayer deposition, at which point the initial ad-layer is compressed 2.8% relative to bulk lead. Because of this strain, lead is not deposited epitaxially on this template, but instead grows in multi-level islands oriented in the direction normal to the substrate but randomly misoriented in the plane of the substrate. The initial

underpotentially deposited monolayer reconstructs after the deposition of approximately 5 "equivalent monolayers" of bulk lead. This apparently relieves the stress resulting from the lattice mismatch between the compressed monolayer and the bulk deposit. The deposition of a relatively thick layer, such as 100 equivalent monolayers, results in a (111) fiber texture structure.

ACKNOWLEDGEMENTS

This work was partially supported by the Office of Naval Research and by the Department of Energy, Office of Basic Energy Sciences, Division of Materials Sciences under contract No. DE-AC03-76SF00098. All the experiments were conducted at Stanford Synchrotron Radiation Laboratory (SSRL) which is supported by the Department of Energy, Office of Basic Energy Sciences, Chemical Sciences Division. We thank Professor J. Krim for many useful discussions.

REFERENCES

1. See for example: D. Kolb in *Advances in Electrochemistry* H. Gerischer and C. Tobias, Eds., Vol. II, Wiley, New York, 1978, p. 125.
2. K. Takayanagi, D. Kolb, K. Kambe, and G. Lehmpfuhl, *Surf. Sci.*, **100**, 407 (1980).
3. R. Corn, M. Romagnoli, M. Levenson, and M. Philpott, *J. Chem. Phys.*, **81**, 4127 (1984).; G. Richmond, *Langmuir*, **2**, 132 (1986).
4. G. Materlik, J. Zenhagen and W. Uelhoff, *Phys. Rev. B* **32** (1985) 5501; G. Materlik, M. Schmah and J. Zegenhagen, *Ber. Bunsenges. Phys. Chem.* **91** (1987) 292.
5. L. Blum, H. Abruna, J. White, J. Gordon, G. Borges, M. Samant, and O. Melroy, *J. Chem. Phys.*, **85**, 6732 (1986).
6. M. Samant, G. Borges, J. Gordon, L. Blum, and O. Melroy, *J. Am. Chem. Soc.*, **109**, 5970 (1987).
7. R. Muller and J. Farmer, *Surf. Sci.*, **135**, 521 (1983).
8. J. Gordon and S. Ernst, *Surf. Sci.*, **100**, 499 (1980).
9. R. Chang and T. Furtak, *Surface Enhanced Raman Scattering*, Plenum Press, New York, 1982.
10. K. Kinimatsu, H. Seki, W. Golden, J. Gordon, and M. Philpott, *Langmuir*, **2**, 464 (1986).
11. A. Hubbard, *Acc. Chem. Res.*, **13**, 177 (1980).
12. P. Ross and F. Wagner, *Adv. in Electrochem. and Electrochem. Eng.* Vol. 13, H. Gerischer and C. Tobias eds., Wiley-Interscience (New York), 1984, pp. 69-112.

13. J. Matthews, *Epitaxial Growth*, Academic Press, New York, 1975.
14. R. Pandit, M. Schick, and M. Wortis, *Phys. Rev. B* 26, 5112 (1982).
15. M. Bienfait, J.L. Suzanne, E. Lerner, J. Krim, and J. Dash, *Phys. Rev. B* 29, 983 (1984).
16. F. Gittes and M. Schick, *Phys. Rev. B* 30, 209 (1984); C. Ebner, C. Rottamn, and M. Wortis, *Phys. Rev. B* 28, 4186 (1983).
17. M. Samant, M. Toney, G. Borges, L. Blum, O. Melroy, *J. Phys. Chem.* 92, 220 (1988).
18. M. Samant, M. Toney, G. Borges, L. Blum, O. Melroy, *Surface Sci.* 193, L29 (1988).
19. R. Chianelli and J. Scanlon, *J. Electrochem. Soc.*, 125, 1563 (1978).
20. J. Dahn, M. Py, and R. Haering, *Can. J. Phys.*, 60, 307 (1982).
21. M. Fleischmann, A. Oliver, and R. Robinson, *Electrochim. Acta*, 31, 899 (1986).
22. W. Marra, P. Fuoss, and P. Eisenberger, *Phys. Rev. Lett.* 49, 1169 (1982).
23. I. Robinson, *Phys. Rev. Lett.* 50, 1145 (1983).
24. J. Bohr, R. Feidenhansl, M. Nielsen, M. Toney, R. Johnson, and I. Robinson, *Phys. Rev. Lett.* 54, 1275 (1985).
25. M. Nielsen, *Z. Phys. B* 61, 415 (1985).
26. The truncation of a crystal at its surface results in the creation of a significant amount of intensity far away from the Bragg points, which is spread across the Brillouin zone. Measurements of this scattering have recently been reported and were shown to be sensitive to the crystal perfection and surface roughness. These streaks of intensity have been termed crystal truncation rods. The intensity from these rods is of the same order as from an adsorbed monolayer. For a more complete discussion see: I. Robinson, *Phys. Rev. B*, 33 (6), 3830 (1986).
27. The presence of a film of electrolyte of finite thickness (1-10 μ) trapped between the window and the surface in the thin-layer configuration means that lead deposition continues during x-ray analysis and introduces an uncertainty of one or two (1 μ of electrolyte $\approx 3 \times 10^{14}$ atoms/cm²) monolayer equivalents" of deposit for x-ray measurements at potentials cathodic to -550 mV.
28. H. Siegenthaler, K. Juttner, E. Schmidt and W. Lorentz, *Electrochim. Acta* 23 (1978) 1009; H. Siegenthaler and K. Juttner, *Electrochim. Acta*, 24 (1979) 109.

29. E. Bauer, H. Poppa, and G. Todd, *Thin Solid Films* 28, 19 (1975).
30. E. Bauer, *Appl. Surf. Sci.* 11/12, 179 (1982).
31. C. Binns and C. Norris, *Surf. Sci.* 115, 395 (1982).
32. Y. Larher and F. Millot, *J. Phys.*, C4-189 (1977).
33. J. Dash, *Phys. Phys. Rev. B* 15, 3136 (1977).
34. R. Waser and K. Weil, *J. Electroanal. Chem.*, 150, 89 (1983).
35. K. Rawlings, M. Gibson, and P. Dobson, *J. Phys. D: Appl. Phys* 11, 2059 (1978).
36. C. Shaw and S. Fain, *Surf. Sci.* 83, 1 (1979); 91, L1 (1980).
37. J. Unguris, L. Bruch, E. Moog, and M. Webb, *Surf. Sci.* 109;522 (1981).
38. J. Dash, "Films on Solid Surfaces", Academic Press, NY., 1975, p. 169.

FIGURE CAPTIONS

- Figure 1. Voltammogram for the deposition of lead on silver(111). Scan rate 20 mV/s; 5×10^{-3} M lead acetate in 0.1M sodium acetate, 0.1M acetic acid (vs. Ag/AgCl (3M KCl)). Arrow marks the potential for bulk lead deposition in this electrolyte.
- Figure 2. LEED pattern for the hexagonal twist structure¹⁷ of the Pb monolayer on Ag(111) with the (hk) and (hkl) reflections from the overlayer and substrate, respectively, indicated. Arrows show regions of reciprocal space probed by radial (Q) and azimuthal (ϕ) scans.
- Figure 3. Crystal truncation rod for a silver (111)/solution interface. a) Azimuthal scan at $|Q| = 2.51 \text{ \AA}^{-1}$ and $\alpha = \delta = 0.8^\circ$. b) Radial scan at $\phi = 0^\circ$ and $\alpha = \delta = 0.8^\circ$.
- Figure 4. The (10) reflection of the lead monolayer on silver (111) at -425mV . a) Azimuthal scan at $|Q| = 2.11 \text{ \AA}^{-1}$ and $\alpha = \delta = 0.8^\circ$. b) Radial scan at $\phi = 4.5^\circ$ and $\alpha = \delta = 0.8^\circ$.
- Figure 5. Lead-lead near neighbor distance vs. electrode potential. Arrow marks the potential for bulk lead deposition in this electrolyte.
- Figure 6. Radial scan ($\phi = 0.0^\circ$ and $\alpha = \delta = 0.8^\circ$) of the lead (220) reflection for a silver (111) electrode on which 30 mC/cm^2 (about 100 'equivalent' monolayers) of lead has been deposited.

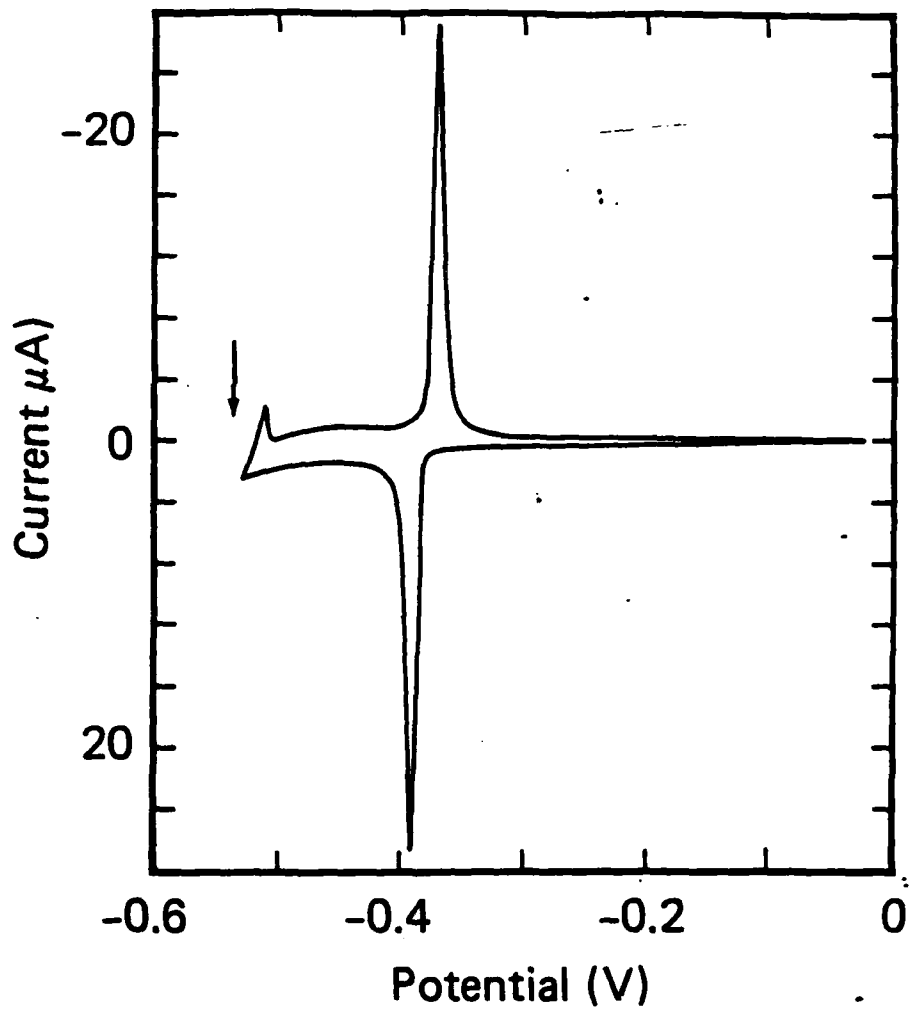
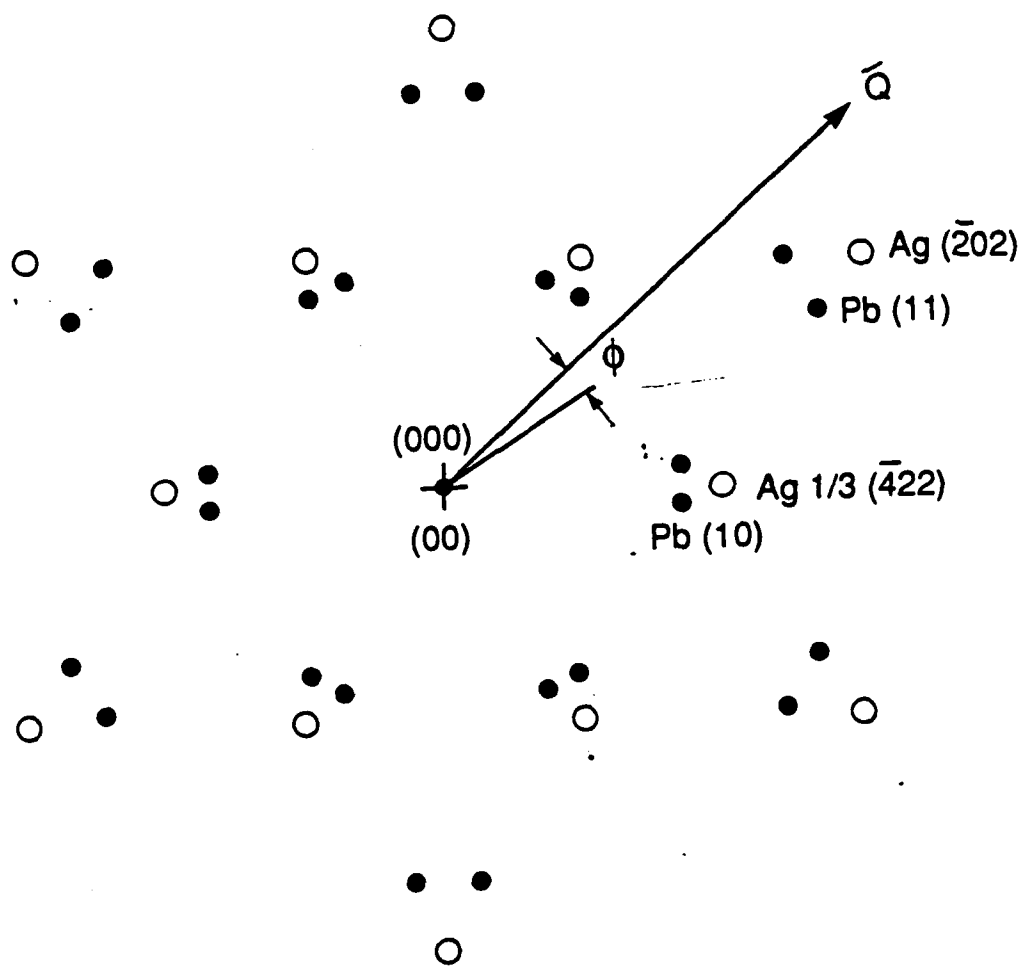


Fig. 1



XBL 887-8919

Fig. 2

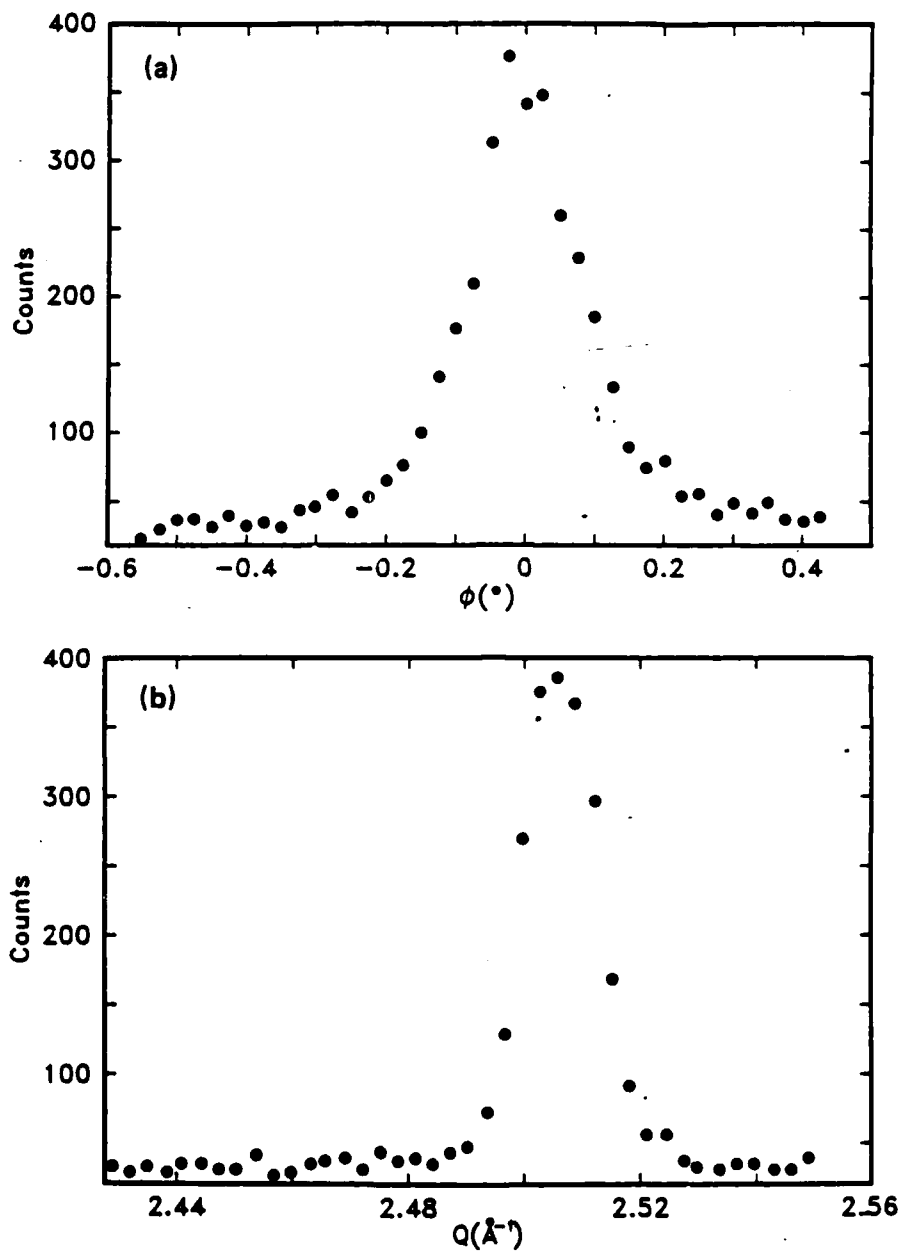
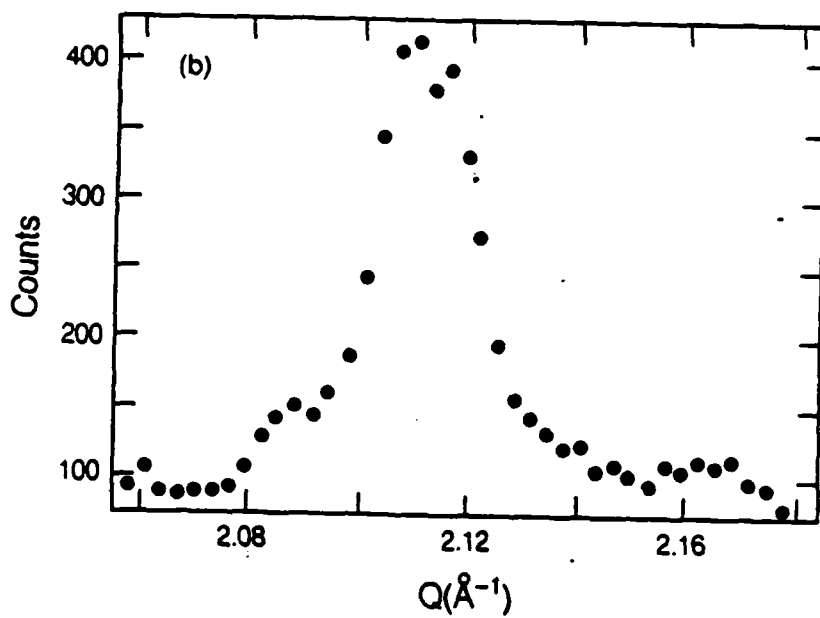
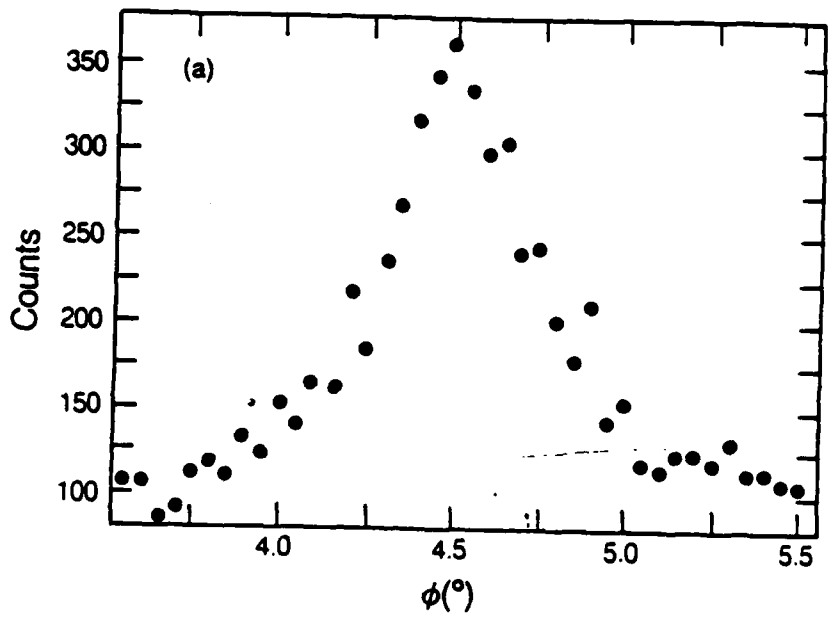
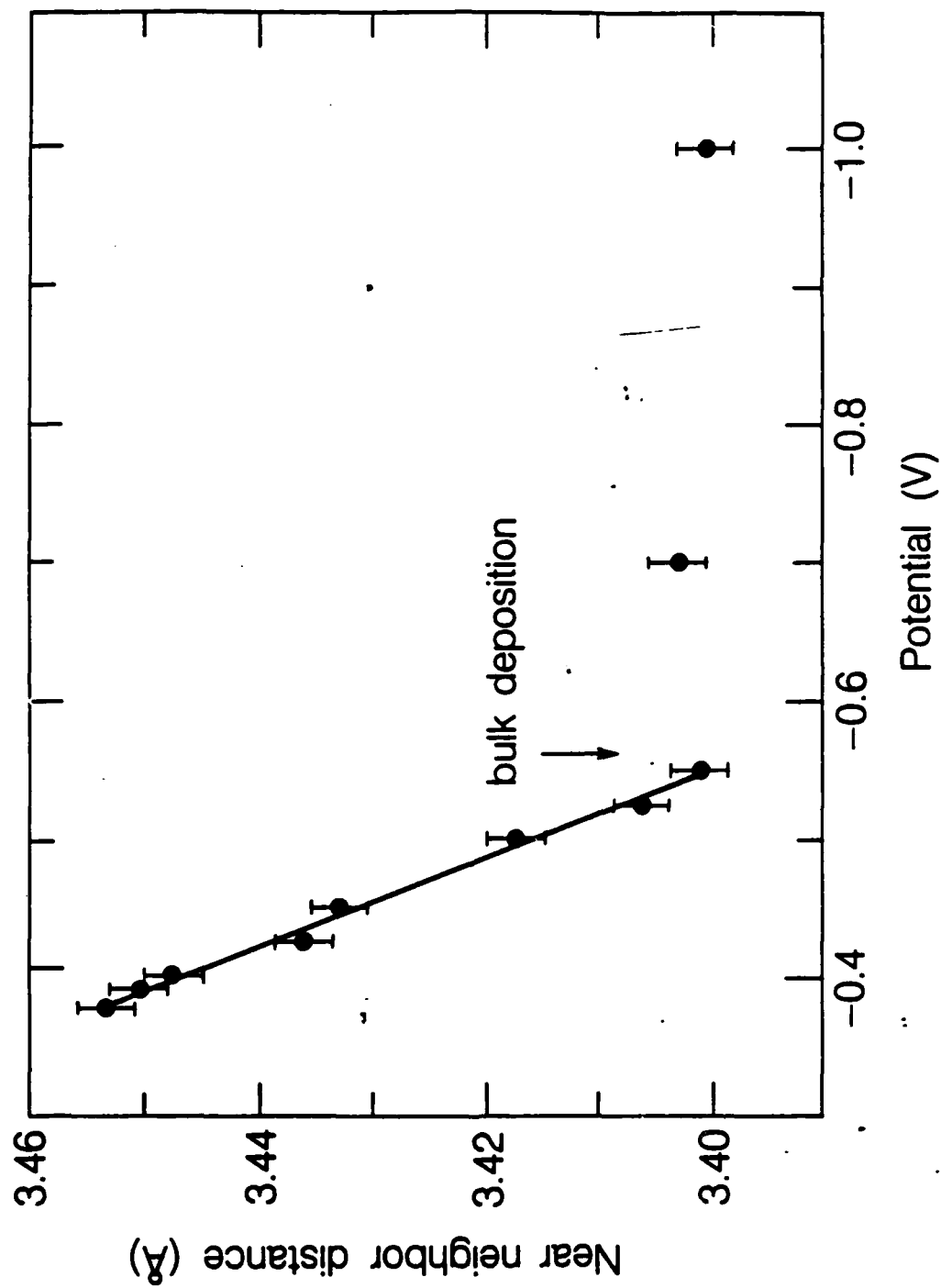


Fig. 3



XBL 888-9267

Fig. 4



XBL 8712-5761

F.g. 5

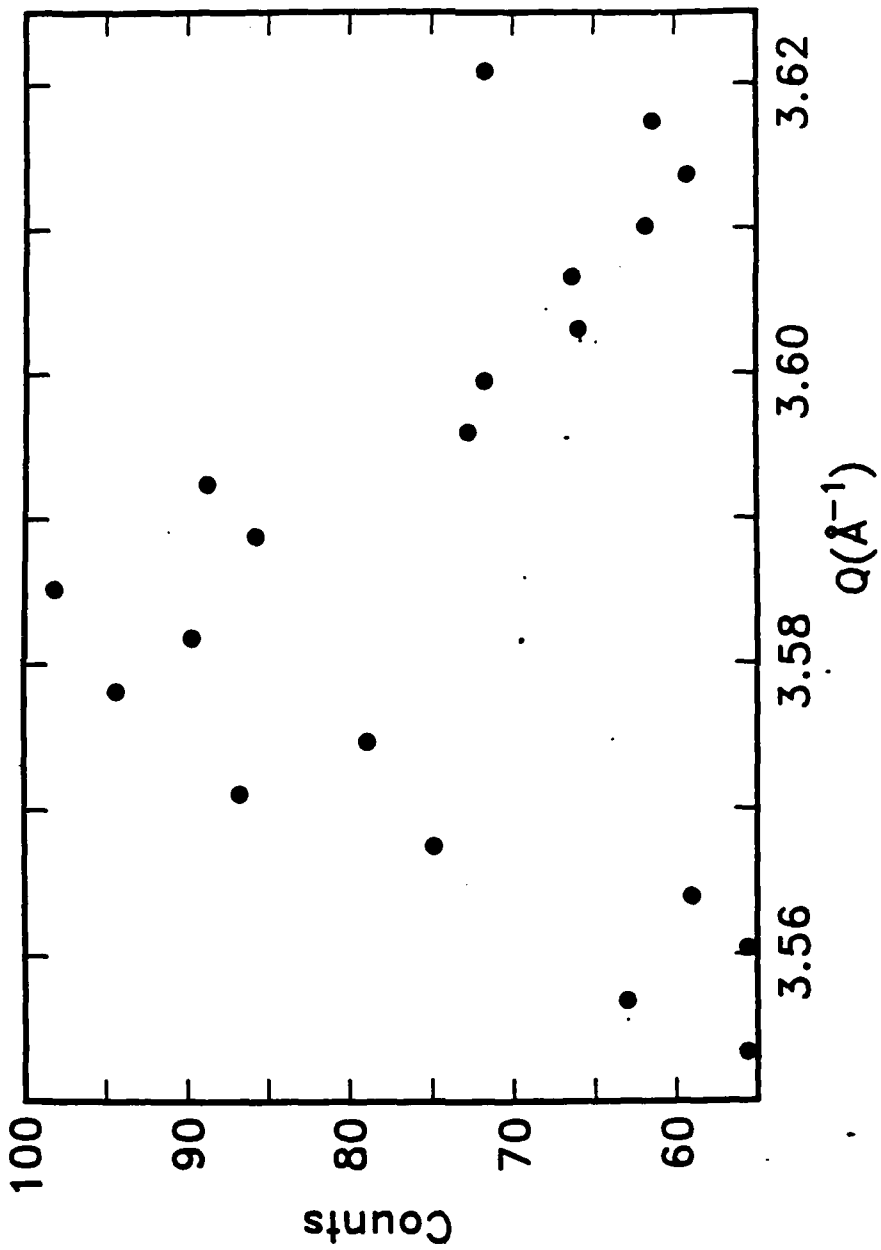


Fig. 6